Reactive oxygen species mediate the down-regulation of mitochondrial transcripts and proteins by tumour necrosis factor-α in L929 cells

José A. SÁNCHEZ-ALCÁZAR*[1], Erasmus SCHNEIDER†, Inmaculada HERNÁNDEZ-MUÑOZ‡, Jesús RUIZ-CABELLO§, Eva SILES-RIVAS‡, Paz DE LA TORRE‡, Belen BORNSTEIN‖, Gloria BREA*, Joaquín ARENAS‡, Rafael GARESSE‖, José A. SOLÍS-HERRUZO‡, Alan J. KNOX¶ and Plácido NAVAS*

*Laboratorio Andaluz de Biología, Universidad Pablo de Olavide, Carretera de Utrera Km 1, Sevilla 41013, Spain, †Wadsworth Center, Empire State Plaza, Albany, NY 12201, U.S.A., ‡Centro de Investigación, Hospital Universitario "12 de Octubre", Madrid, Spain, §Departamento de Química-Física II, Unidad RNM, Facultad de Farmacia, Universidad Complutense, Madrid, Spain, ‖Facultad de Medicina & Departamento de Bioquímica, Instituto de Investigaciones Biomédicas "Alberto Sols" CSIC-UAM, Universidad Autónoma de Madrid, Madrid, Spain, and ¶Clinical Sciences Building, City Hospital, Hucknall Road, Nottingham NG5 1PB, U.K.

In this study, we show that reactive oxygen species production induced by tumour necrosis factor α (TNF-α) in L929 cells was associated with a decrease in the steady-state mRNA levels of the mitochondrial transcript ATPase 6-8. Simultaneously, the transcript levels of two nuclear-encoded glycolytic enzymes, glyceraldehyde-3-phosphate dehydrogenase (GAPDH) and phosphofructokinase, were increased. These changes were associated with decreased protein levels of the ATPase subunit *a* (encoded by the mitochondrial ATPase 6 gene) and cytochrome *c* oxidase subunit II, and increased protein levels of phosphofructokinase. Since TNF-α had no effect on the amount of mitochondrial DNA, the results suggested that TNF-α acted at the transcriptional and/or post-transcriptional level. Reactive oxygen species scavengers, such as butylated hydroxianisole and butylated hydroxytoluene, blocked the production of free radicals, prevented the down-regulation of ATPase 6-8 transcripts, preserved the protein levels of ATPase subunit *a* and cytochrome *c* oxidase subunit II, and attenuated the cytotoxic response to TNF-α, indicating a direct link between these two phenomena.

Key words: ATPase 6-8, free radical, glycolysis, mitochondrial transcript, necrosis, tumour necrosis factor α (TNF-α).

INTRODUCTION

Tumour necrosis factor α (TNF-α) is a cytokine, produced mainly by activated macrophages [1], with cytotoxic effects against certain tumour cells [2]. Although these effects have been studied extensively, the molecular mechanism of action of TNF-α is not well understood [3,4]. Previous investigations have shown contradictory results regarding whether TNF-α-induced cytotoxicity occurs through necrosis or apoptosis [3]. Recent results indicate that TNF-α induces necrosis in L929 cells, although apoptosis-like features have also been observed [5,6]. Regardless of the mode of cell death, however, it has been shown that TNF-α-induced cytotoxicity of L929 cells is mediated by mitochondrial formation of reactive oxygen species (ROS) [5–9]. The reported ability of antioxidants to protect cells against TNF-α cytotoxicity supports this hypothesis [7,10]. Exposing cells to oxidative stress can result in severe metabolic dysfunction, including the peroxidation of lipid membranes [11], an increase of cytosolic Ca^{2+} [12], induction of mitochondrial inner-membrane permeability transition [13] and DNA damage [14,15]. In cells exposed to oxidative stress, there are two primary effects: direct molecular damage, such as lipid peroxidation, and induction of protective systems that repair and protect the cell against additional damage [16–18]. The latter response includes both antioxidant enzymes and damage-removal and -repair systems for oxidatively damaged lipids, proteins and DNA. Mitochondria have been found to be especially sensitive to oxidative damage. Release of calcium, depletion of ATP, lipid peroxidation, protein oxidation, DNA damage and loss of electron-transport capacity have all been reported [13,19–24]. Several lines of evidence also suggest that oxidative stress decreases mitochondrial transcription and steady-state levels of mitochondrial RNAs [25–28]. Modulation of mitochondrial expression by free radicals is not limited to RNA, as certain mitochondrial proteins are also specifically degraded in response to oxidative stress [20].

The objective of this study was to investigate the effects of TNF-α-mediated free radical production on mitochondrial transcripts and protein levels in L929 cells, and to determine its relationship with cell death. We show here that ROS production induced by TNF-α in L929 cells was associated with a decrease in the steady-state mRNA levels of the mitochondrial transcript ATPase 6-8 in a time-dependent manner. Simultaneously, the transcript levels of two nuclear-encoded glycolytic enzymes, glyceraldehyde-3-phosphate dehydrogenase (GAPDH) and phosphofructokinase (PFK), were increased. These changes were associated with decreased levels of the mitochondrial DNA (mtDNA)-encoded proteins ATPase subunit *a* (encoded by the mitochondrial ATPase 6 gene) and cytochrome *c* oxidase, subunit II (COX II), and increased protein levels of PFK. Furthermore, ROS scavengers such as butylated hydroxianisole (BHA) and butylated hydroxytoluene (BHT) blocked the production of free

Abbreviations used: BHA, butylated hydroxianisole; BHT, butylated hydroxytoluene; COX II, cytochrome *c* oxidase, subunit II; GAPDH, glyceraldehyde-3-phosphate dehydrogenase; MnSOD, manganese superoxide dismutase; mtDNA, mitochondrial DNA; PFK, phosphofructokinase; PI, propidium iodide; R123, Rhodamine 123; ROS, reactive oxygen species; TCA, tricarboxylic acid; TMPD, tetramethyl-*p*-phenylenediamine; TNF-α, tumour necrosis factor α; TSP, sodium 3-trimethylsilyl-(2,2,3,3-$^2H_4$)-propionate.

[1] To whom correspondence should be addressed (e-mail jasanalc@dex.upo.es).

radicals, prevented the down-regulation of ATPase 6-8 transcripts, and ATPase subunit *a* and COX II protein levels, and attenuated the cytotoxic response to TNF-α. These results indicate that down-regulation of mitochondrial proteins by free radicals might be implicated in TNF-α-mediated cytotoxicity in L929 cells.

EXPERIMENTAL

Materials

Recombinant human TNF-α was purchased from Genzyme Co. (Cambridge, MA, U.S.A.). RPMI-1640 medium was from Biochrom (Berlin, Germany). Propidium iodide (PI) and trypsin were purchased from Sigma (Alcobendas, Madrid, Spain). Dihydrorhodamine 123, Hoechst 33342, anti-cytochrome *c* oxidase (subunit II), anti-ubiquinol-cytochrome *c* oxidoreductase subunit core 2, anti-ATPase α antibodies and high-fluorescence FITC-labelled goat anti-mouse antibodies were purchased from Molecular Probes (Eugene, OR, U.S.A.). Anti-PFK antibodies were from Biodesign International (Saco, ME, U.S.A.). Anti-cytochrome *c* antibodies (7H8.2C12 and 6H2.B4) were purchased from BD PharMingen (San Diego, CA, U.S.A.). Anti-GAPDH monoclonal antibody, clone 6C5, was purchased from Research Diagnostic (Flanders, NJ, U.S.A.). A cocktail of protease inhibitors (complete cocktail) was purchased from Roche Biochemicals (Indianapolis, IN, U.S.A.). The ECL Western blotting analysis system was from Amersham Biosciences (Little Chalfont, Bucks., U.K.). Anti-manganese superoxide dismutase (MnSOD) antibodies were a gift from Dr Jose A. Melendez (Albany Medical College, Albany, NY, U.S.A.). PFK cDNA was a gift from Dr Juan J. Aragón (Universidad Autónoma de Madrid, Madrid, Spain). 18 S rDNA was a gift from Dr Michael P. King (Thomas Jefferson University, Philadelphia, PA, U.S.A.). Anti-ATPase 6 (subunit *a*) antibodies and the clone pAM I were a gift from Dr David A Clayton (Stanford University, Stanford, CA, U.S.A.).

Cell cultures

Cells from the murine fibrosarcoma cell line L929 (American Type Culture Collection, Rockville, MD, U.S.A.) were grown in RPMI-1640 medium supplemented with 10 % heat-inactivated fetal calf serum, 2 mM glutamine, penicillin (100 units/ml) and streptomycin (0.1 mg/ml) in a humidified incubator in 5 % CO_2 in air, at 37 °C.

Separation of viable and dead cells

During the process of cell death, L929 cells detached from the flask and floated in the medium. In this study, we exploited this phenomenon as an easy way to separate attached/living cells and floating/dead cells. Thus, after various incubation times, the medium containing the non-adherent cells was removed and the cells collected if needed. The monolayer of attached cells was then washed with PBS and incubated with trypsin for 5 min at 37 °C to remove the cells from the flask. Viability of floating and attached cells was determined by PI staining and microscopic visualization. Only samples of attached cells that contained > 85 % viable cells were used for further studies. The floating cell population was 100 % PI-positive.

Cytotoxicity assays

Cytotoxicity was measured using lactate dehydrogenase leakage from damaged cells and was expressed as a percentage of total cellular lactate dehydrogenase activity, as described by Decker and Lohmann-Matthes [29]. Lactate dehydrogenase activity was measured using a commercial assay kit (Cromatest; Laboratorios Knickerbocker, Barcelona, Spain).

Cytochrome *c* oxidase activity

Cells were treated with TNF-α for 72 h. At this time, the attached cells were harvested, centrifuged and resuspended in respiration buffer (0.25 M sucrose, 0.1 % BSA, 10 mM $MgCl_2$, 10 mM K^+Hepes and 5 mM KH_2PO_4, pH 7.2) at a final concentration of 2×10^7 cells/ml. An aliquot (0.5 ml) of the suspension was injected into a chamber containing 3.5 ml of air-saturated respiration buffer and 1 mM ADP at 37 °C. The cells were permeabilized with digitonin (final concentration, 0.005 %), and substrates and inhibitors were added in the following order and final concentrations: 50 nM antimycin A, 1 mM ascorbate and 0.4 mM tetramethyl-*p*-phenylenediamine (TMPD). Antimycin A was used to inhibit autologous mitochondrial electron transport. TMPD is an electron donor that reduces cytochrome *c* non-enzymically. Therefore, when TMPD is used as a substrate, changes in O_2-uptake rates reflect changes in cytochrome *c* oxidase activity. Ascorbate was used to reduce TMPD. Oxygen concentration was calibrated with air-saturated buffer, assuming 390 ng-atoms of oxygen/ml of buffer. Rates of potassium cyanide-sensitive oxygen consumption are expressed as ng-atoms of oxygen/min per 1×10^7 cells.

Glutamine oxidation

L929 cells were treated with TNF-α for 72 h. After removing the medium and the floating dead cells, the attached cells were incubated in 5 ml of RPMI-1640 containing 2 mM glutamine and 0.5 μCi of L-[U-^{14}C]glutamine (DuPont-New England Nuclear, Boston, MA, U.S.A.) with a specific activity of 216 mCi/mmol. Then 0.2 ml of 6 M KOH was injected into the central wells to trap CO_2. These were small plastic wells situated inside the flasks and above the level of the incubation medium. Flasks were sealed with stoppers and incubated at 37 °C for 3 h. CO_2 evolved during the incubation was trapped by the central wells. Incubation was stopped by adding 0.2 ml of 2 M perchloric acid through the rubber cap into the flasks. After 2 h, the central wells were transferred to plastic scintillation vials containing 1 ml of water and 15 ml of scintillation fluid and placed in a scintillation counter for radioactivity measurements. Results are expressed as c.p.m./10^6 cells.

ATP assay

Cellular content of ATP in the attached/living population were measured in trichloroacetic acid (10 %, w/v)-precipitated samples using the luciferin/luciferase reaction with an ATP bioluminescent assay kit (Sigma). Luminescence was measured in a bioluminometer equipped with an injector (Lumat LB 9501; Berthold).

Cell extracts and NMR spectroscopy

Cell extracts were prepared from 60×10^6 attached/living L929 cells. Harvested cells were centrifuged at 4 °C three times in Hepes-buffered Hanks's balanced salt solution containing 0.1 % (w/v) dextrose. The cell pellet was treated with five vol. of cold trichloroacetic acid 10 % (w/v), followed by sonication on ice for 5 min. The extract was neutralized by 4 M KOH, the mixture was centrifuged for 30 min at 15000 ***g*** (4 °C) and the supernatant was lyophilized and stored at −80 °C. For NMR measurements, the dried homogenate was dissolved in 0.7 ml of ^2H_2O in a 5 mm

NMR tube. The pH was adjusted with ^{2}HCl to pH 7.4. High-resolution ^{1}H-NMR spectra were obtained at 500 MHz using a vertical superconducting narrow-bore Bruker DBX-500 spectrometer (Ettlingen, Germany). The magnetic field homogeneity was optimized by an automatic shimming programme, and water linewidths of typically 3 Hz were obtained. Spectra were collected using presaturation at the frequency of the residual proton/deuterium oxide (HOD) peak followed by a 45° flip angle pulse, with an interpulse time of 3.5 s for full relaxation of all the resonances. Scans (128) were accumulated for each cell extract spectrum. Proton spectra were standardized by referencing to TSP [sodium 3-trimethylsilyl-(2,2,3,3-$^2H_4$)-propionate]. The spectra were analysed on a personal computer running commercial Bruker Win-NMR software. The data were zero-filled, line broadened and then Fourier-transformed. Zero-order phasing and baseline correction was performed. We measured peak areas with the same software under the interactive deconvolution package. Initial starting values for the peaks were defined manually and then fitted automatically with Lorentzian lines. Quantitative analysis of identified peaks was carried out by calculating peak-height ratios relative to TSP.

Glucose and lactate determinations

Glucose and lactate concentrations in the medium from control and TNF-α-treated cells were measured using commercial assay kits (Sigma).

Northern blot analysis

RNA was isolated from the attached/living cells by the phenol/chloroform extraction method of White and Bancroft [30]. Total RNA (10 μg) was electrophoresed in a 1% agarose/2.2 M formaldehyde gel in 20 mM Mopso [3-(*N*-morpholino)-2-hydroxypropanesulphonic acid] buffer, pH 7.0. RNA samples were stained with ethidium bromide and transferred overnight by capillary blotting in 20 × SSC (where 1 × SSC is 0.15 M NaCl/0.015 M sodium citrate) to nylon membranes. The RNA was UV-crosslinked to the membranes and prehybridized at 65 °C in 7% SDS plus 0.5 M phosphate buffer (pH 7.0) and 50 μg/ml sonicated salmon sperm DNA. The nylon membranes were hybridized overnight at 65 °C in freshly prepared hybridization solution with addition of 1×10^6 c.p.m./ml of the labelled cDNA probe. The nylon membranes were washed at a stringency of 2 × SSC/0.1% SDS at 65 °C for 15 min and exposed to X-ray film at −70 °C with an intensifying screen. The radiograms were quantified by scanning laser densitometry (Desk Top™ Scanner Plus; Amersham Biosciences) and the absorbances of each specific signal were normalized with the corresponding value obtained for the 18 S rDNA.

ATPase 6 probe generation

A specific DNA fragment covering most of the ATPase 6 gene was excised from pAM I and cloned into the pBluescript vector (Stratagene, La Jolla, CA, U.S.A.) by standard techniques.

DNA slot-blot analysis

Different amounts of total DNA from control and TNF-α-treated cells for 72 h were blotted to a Zeta-probe membrane using the Manifold II System (Schleicher & Schuell) and fixed to the filter according to the manufacturer's instructions. To quantify the mtDNA, filters were probed at high stringency with an [α-^{32}P]dCTP-labelled mouse pAM I (entire mouse mtDNA) probe. After several washes with 0.1% SDS/0.1 × SSC at 68 °C the filter was autoradiographed.

Measurement of intracellular generation of ROS

Flow-cytometric analysis of the intracellular generation of ROS was performed using dihydrorhodamine 123 as a probe. Cells were cultured in six-well plates (35 mm diameter well) and, at confluence (1×10^6 cells/plate), were treated with TNF-α (25 ng/ml). After the indicated incubation times, dihydrorhodamine 123 (1 μM) was added and the incubation was prolonged for 30 min. Once the incubation was finished, cells were harvested, washed, centrifuged (200 ***g***), resuspended in RPMI-1640 medium and analysed by flow cytometry (excitation at 488 nm and fluorescence detection at 530 nm). Rhodamine 123 (R123) fluorescence was analysed in viable cells characterized by forward scatter versus side scatter.

Measurement of cellular glutathione

Cellular glutathione on attached/living cells was measured using Eady et al.'s modification [31] of Tietze's assay [32], based on the principle that reduced glutathione can be measured by an enzymic recycling procedure in which it is sequentially oxidized by 5,5′-dithiobis-(2-nitrobenzoic acid) and reduced by NADPH in the presence of glutathione reductase. The rate of formation of 2-nitro-5-thiobenzoic acid can be followed using a spectrophotometer and reduced glutathione quantified by reference to a standard curve.

Western blot analysis

Cytosolic and mitochondrial fractions from control and TNF-α-treated cells were prepared as described in [33]. Floating and attached L929 cells were collected separately, washed twice with ice-cold PBS, pH 7.4, followed by centrifugation at 200 ***g*** for 5 min. The cell pellet was then resuspended in 600 μl of extraction buffer containing 220 mM mannitol, 68 mM sucrose, 50 mM Pipes/KOH, pH 7.4, 50 mM KCl, 5 mM EGTA, 2 mM $MgCl_2$, 1 mM dithiothreitol and protease inhibitors (Complete Cocktail; Roche Biochemicals). After 30 min of incubation on ice, cells were homogenized with a Teflon homogenizer (3 min, 300 rev./min). Cell homogenates were spun at 14000 ***g*** for 15 min and supernatants were removed and stored at −70 °C, until analysis by gel electrophoresis. The quality of the cytosolic fraction was routinely monitored by Western blotting for COX II for potential mitochondrial contamination. The quality of the mitochondrial fraction was monitored routinely by Western blotting for GAPDH for potential cytosolic contamination. From whole lysates (50 μg), cytosolic or mitochondrial proteins were separated on a 5 or 12% denaturing SDS/PAGE minigel. Primary antibodies were diluted 1:1000. The membrane was then incubated with the corresponding secondary antibody coupled to horseradish peroxidase at a 1:10000 dilution. The specific protein complexes were identified using the ECL Western blotting analysis system.

Cytochrome *c* immunocytochemistry

L929 cells were grown on 1 mm glass coverslips (Goldseal No. 1) for 24–48 h in RPMI-1640 containing 10% fetal bovine serum. Cells were then treated with TNF-α for 72 h. To differentiate between live and dead cells, the 'Dead Red' reagent (Molecular Probes) was added to the cells 10 min before fixation. For immunostaining cells were fixed in 3.8% paraformaldehyde for 5 min at room temperature, permeabilized in 0.1% saponin for 5 min and stained with anti-cytochrome *c* antibodies (6H2.B4) diluted 1:100 in PBS for 1–2 h at 37 °C in a humidified

chamber. Excess antibody binding was removed by washing the coverslips with PBS three times for 5 min each. The secondary antibody, a high-fluorescence FITC-labelled goat anti-mouse antibody, diluted 1:100 in PBS, was added and incubated for 1 h 37 °C. Coverslips were then rinsed with PBS for 3 min, incubated for 1 min with PBS containing Hoechst 33342 (1 μg/ml) and washed with PBS three times for 5 min each. Finally, the coverslips were mounted on to microscope slides using Vectashield mounting medium (Vector Laboratories, Burlingame, CA, U.S.A.) and analysed using an Olympus BX40 fluorescent microscope using a $\times 1000$ final magnification.

Statistical analysis

All results are expressed as means $\pm$ S.D. unless stated otherwise. Unpaired Student's t tests were used to evaluate the significance of differences between groups, accepting $P < 0.05$ as the level of significance.

RESULTS

Treatment with TNF-α alone induces a necrosis-like mode of death in L929 cells

The L929 mouse fibrosarcoma cell line is commonly used to test the cytotoxic effects of TNF-α [34–37]. However, contradictory reports exist regarding the kind of cell death induced by TNF-α in L929 cells. Previously, we have shown that TNF-α in the presence of cycloheximide induces in L929 cells a kind of cell death with many features of the apoptotic programme: membrane blebbing, cytochrome c release, caspase activation, chromatin condensation and nuclear fragmentation [38]. To ascertain whether L929 cells treated with TNF-α alone underwent apoptosis or necrosis, we examined cytochrome c release, nuclear morphology and plasma membrane integrity in control and TNF-α-treated cells for 72 h. To check plasma membrane integrity, we used the Dead Red dye, which is a cell-impermeant red fluorescent nucleic acid stain that labels only cells with a disrupted membrane [39]. By using this stain, viability staining can take place before fixation without altering the distinctive immunofluorescence-staining pattern. Untreated L929 cells showed intact plasma membranes, a punctuate pattern for cytochrome c, consistent with its mitochondrial localization, and uniformly stained nuclei (Figure 1). In TNF-α-treated cells, we analysed both the attached/living cells and the floating/dead cells. In the attached/living population, the cells showed intact plasma membranes, a punctuate pattern for cytochrome c and uniformly stained nuclei. In contrast, the floating/dead cells showed disruption of the plasma membrane, the almost complete disappearance of cytochrome c staining and the presence of relatively intact nuclei. Jurkat cells that undergo extensive

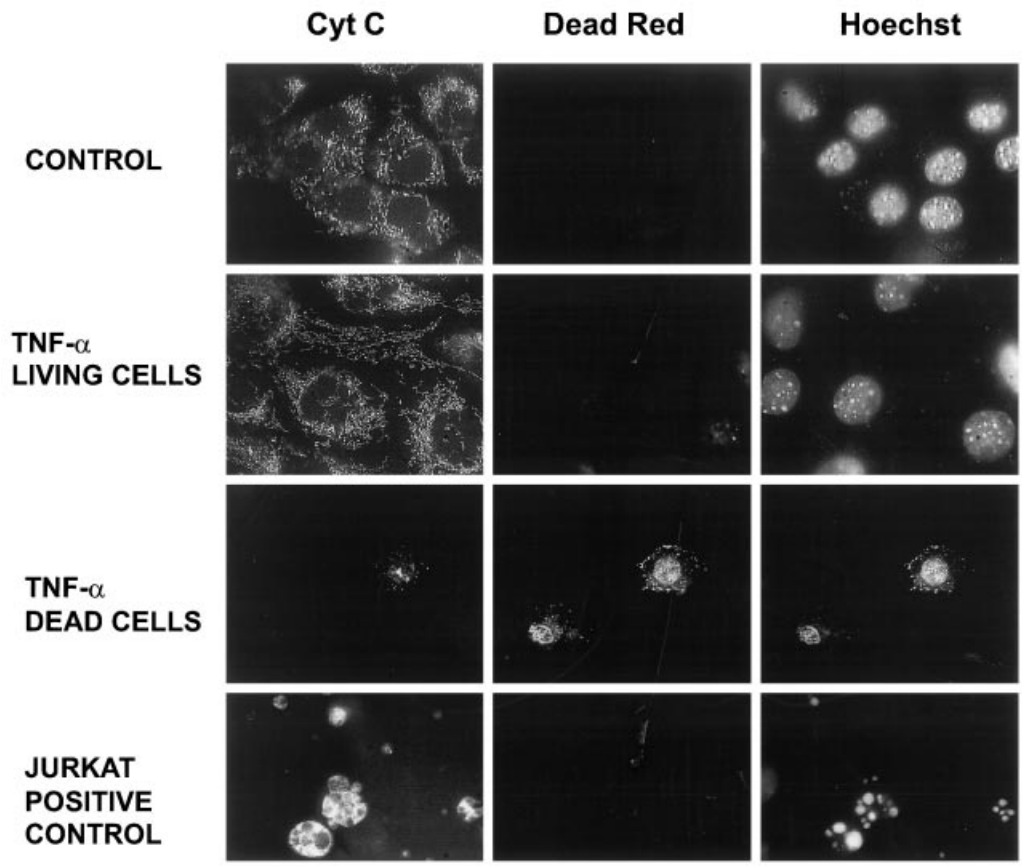

Figure 1 TNF-α induces necrosis in L929 cells

Immunolocalization of cytochrome c (Cyt C), plasma membrane permeability (Dead Red) and nuclear morphology (Hoechst) are shown in control and TNF-α-treated L929 cells (floating and attached cells). Cells were grown on glass coverslips and treated with 25 ng/ml TNF-α for 72 h, fixed and immunostained with anti-cytochrome c monoclonal antibodies (clone 7H8C12) as described in the Experimental section. Jurkat cells treated with camptothecin (10 μM) were used as a positive control for apoptosis.

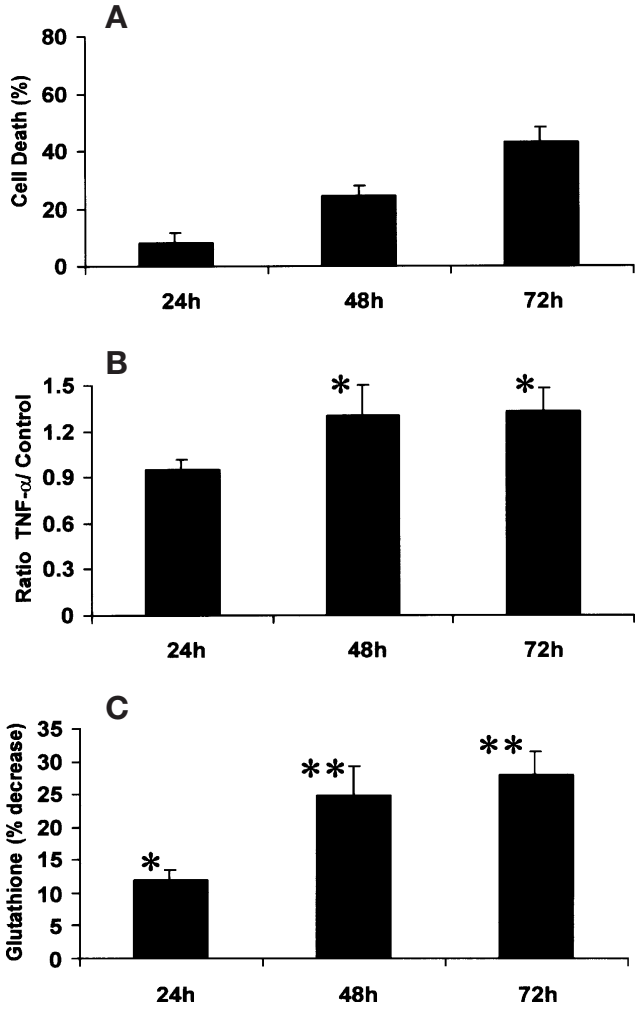

Figure 2 Effect of TNF-α on cellular viability, intracellular generation of ROS and glutathione levels

Cells were incubated in the absence or presence of 25 ng/ml TNF-α for 24, 48 and 72 h. (**A**) Cell viability was examined as described in the Experimental section. (**B**) Cellular generation of ROS was determined by flow cytometry using R123 fluorescence. (**C**) Effect of TNF-α on the intracellular concentration of glutathione. Results are means $\pm$ S.D. from three independent experiments. $^{*}P < 0.01$, $^{**}P < 0.001$ between control and treated cells. In (**A**) and (**C**), data represent the percentage increase or decrease with respect to controls.

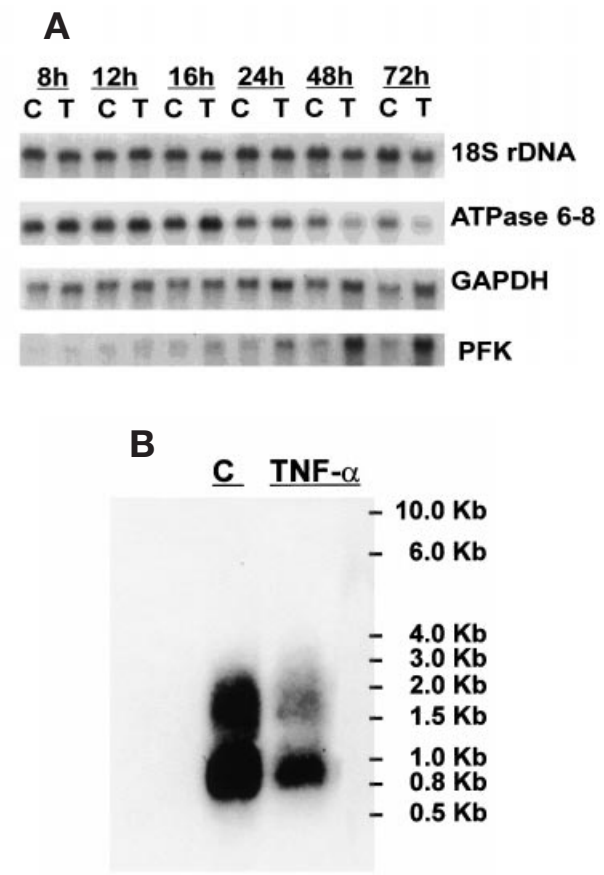

Figure 3 TNF-α regulation of both mitochondrial and nuclear gene expression in L929 cells

(**A**) Total RNA (10 μg/lane) isolated from control and TNF-α-treated L929 cells cultured for 8, 12, 16, 24, 48 and 72 h was analysed by Northern hybridization using radiolabelled ATPase 6-8, GAPDH and PFK cDNA probes. Control for RNA loading and integrity was assessed by probing with 18 S rDNA. Representative radiograms are shown; C, control; T, TNF-α. (**B**) Total RNA (10 μg/lane) isolated from control and TNF-α-treated L929 cells cultured for 72 h, was analysed by Northern hybridization using the radiolabelled pAM I probe. A representative radiogram is shown.

apoptotic cell death in response to camptothecin were used as a positive control for apoptosis. As seen in Figure 1, Jurkat cells treated with camptothecin showed a diffuse pattern of cytochrome *c* staining, consistent with its release into the cytoplasm, chromatin condensation and nuclear fragmentation, all in the presence of intact plasma membranes. These observations suggest that the treatment with TNF-α alone induced necrotic cell death in L929 cells.

TNF-α induces cell death and free radical production in L929 cells

It has been reported that TNF-α-induced cytotoxicity in L929 cells is caused by the induced ROS production in mitochondria [7]. Therefore, we examined cell death and ROS levels in control and TNF-α-treated L929 cells. Figure 2(A) shows that murine L929 cells are susceptible to the cytotoxic action of TNF-α. TNF-α caused a 50 % loss of viability after 72 h of treatment. To examine the role of free radicals in TNF-α-induced cytotoxicity, the intracellular generation of ROS by cultured L929 cells in response to TNF-α treatment was measured by flow cytometry using the dihydrorhodamine 123 probe. As shown in Figure 2(B), treatment of cells with 25 ng/ml TNF-α for 48 and 72 h resulted in a significant increase in R123 fluorescence, indicating ROS generation. To investigate the antioxidant reserves under TNF-α treatment, we analysed the levels of glutathione. TNF-α treatment for 24, 48 and 72 h resulted in a significant decrease in total glutathione (Figure 2C), suggesting that TNF-α-induced ROS production was overcoming the cellular defence against free radicals.

Effects of TNF-α on mitochondrial and nuclear mRNA levels

There is compelling evidence suggesting that oxidative stress can modulate the levels of both mRNA and proteins in target cells [22,40]. To examine whether the steady-state levels of mitochondrial and nuclear transcripts were affected by TNF-α-induced free radicals, we studied the effects of TNF-α on the

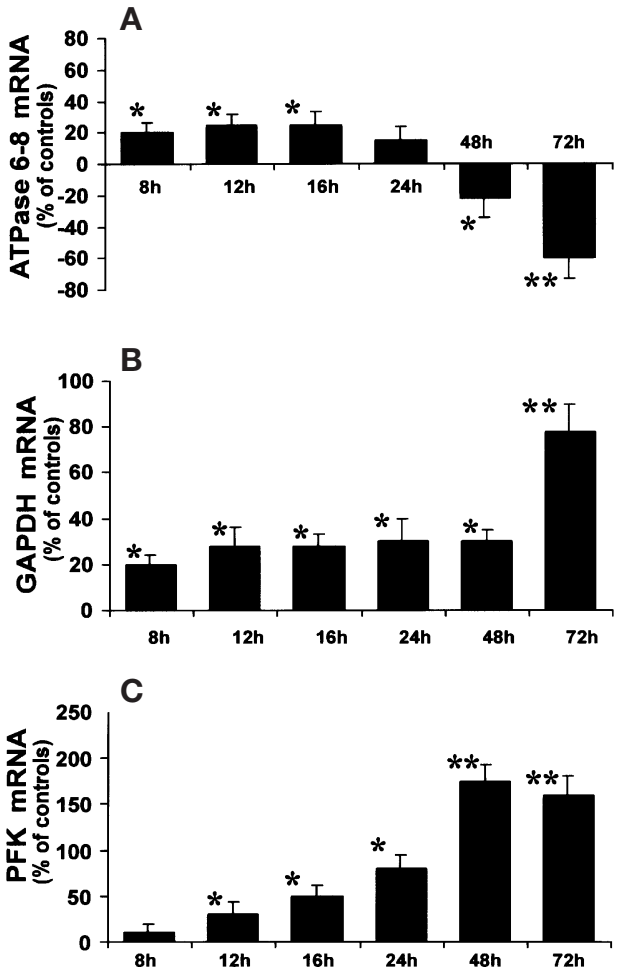

Figure 4 Effect of TNF-α in the content of ATPase 6-8, GAPDH and PFK mRNA in L929 cells

RNA levels were determined by densitometric analysis of three different Northerns blots. The hybridization signals were quantified by laser scanning and normalized to the 18 S rDNA signal. Results are expressed as mean ± S.D. $^{*}P < 0.01$ and $^{**}P < 0.001$ between control and treated cells.

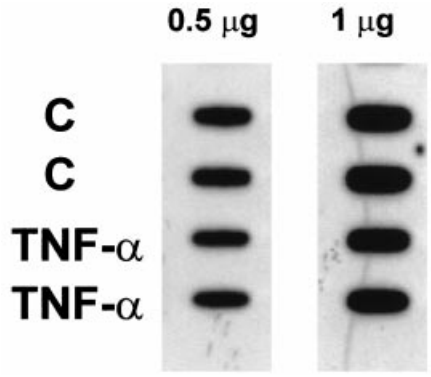

Figure 5 Effect of TNF-α on mtDNA content in L929 cells

Different amounts of DNA isolated from control (C) or TNF-α-treated cells for 72 h were loaded on to nylon membranes and hybridized with pAM I as described in the Experimental section.

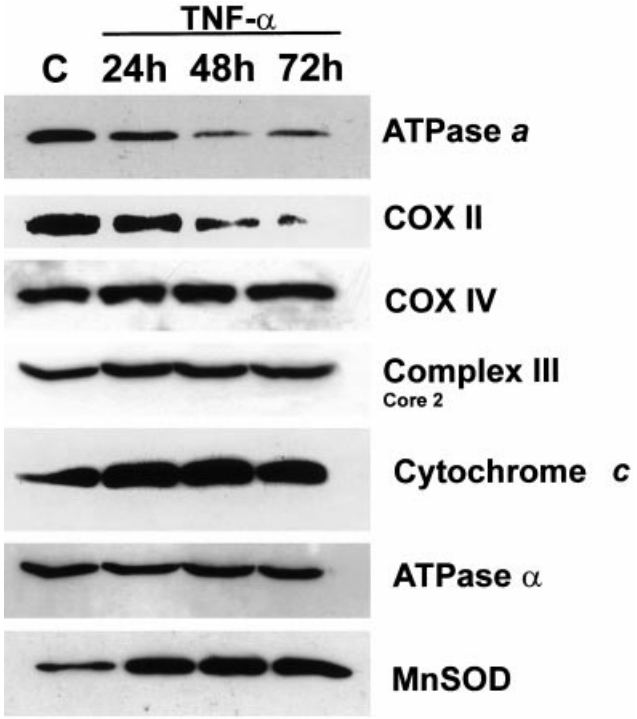

Figure 6 Effect of TNF-α on mitochondrial protein levels

Proteins from mitochondrial extracts of L929 cells exposed to TNF-α (25 ng/ml) for 24, 48 and 72 h, were separated by SDS/PAGE (10% gel) and immunostained with antibodies against ATPase subunits *a* and α, cytochrome *c* oxidase (COX) subunits II and IV, ubiquinol-cytochrome *c* oxidoreductase subunit core 2, MnSOD and cytochrome *c*.

expression of the mitochondrial gene ATPase 6 and the nuclear genes GAPDH and PFK by Northern blot analysis. The ATPase 6 mRNA was detected as the bicistronic mRNA ATPase 6-8 coding for the ATPase 6 and ATPase 8 proteins. TNF-α treatment had a biphasic effect on mRNA expression levels (Figures 3A and 4). During the first 24 h of treatment, TNF-α induced a slight increase in ATP 6-8, GAPDH and PFK mRNA steady-state levels. In a second phase, starting at 48 h, coinciding with ROS generation and the onset of cell death, TNF-α markedly diminished the steady-state levels of the mitochondrial ATPase 6-8 mRNA, whereas it induced a dramatic increase of the nuclear transcripts for GAPDH and PFK.

To determine whether TNF-α had a more general effect on the mRNAs encoded by the mtDNA, we performed Northern Blot analysis of control and TNF-α-treated L929 cells using as a probe the entire mitochondrial genome (probe pAM I). As shown in Figure 3(B), the treatment with TNF-α induced a significant decrease in all the mitochondrial transcripts detected by the pAM I probe, suggesting that TNF-α had a more general effect on the steady-state levels of mitochondrial transcripts.

Effects of TNF-α on mtDNA content in L929 cells

To investigate whether the decrease in ATPase 6-8 mRNA observed in L929-treated cells was due to a reduction in the number of mitochondria per cell, we examined the effects of TNF-α on mtDNA content in L929 cells. Total DNA isolated from L929 control and TNF-α-treated cells was probed with the entire mitochondrial genome (probe pAM I). As shown in Figure 5, the amount of mtDNA was unaltered despite the observed

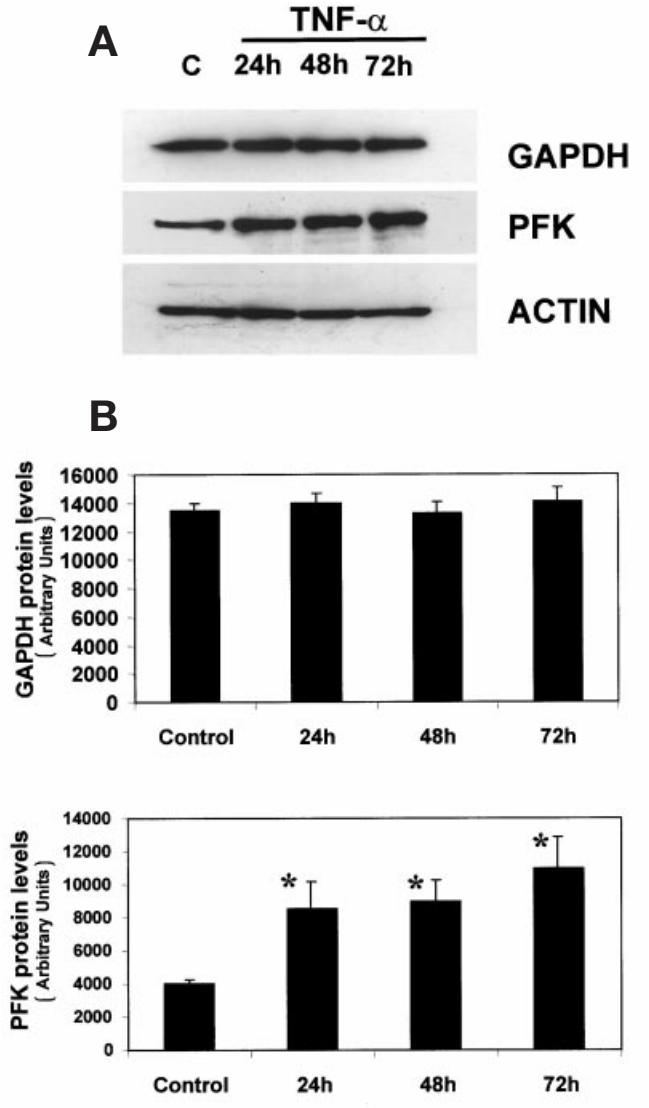

Figure 7 Effect of TNF-α on protein levels of glycolytic enzymes

(**A**) Proteins from cytosolic extracts of L929 cells exposed to TNF-α (25 ng/ml) for 24, 48 and 72 h were separated by SDS/PAGE (10% gel) and immunostained with antibodies against GAPDH and PFK. Actin antibodies were used to check for equal loading. (**B**) Densitometric scanning of GAPDH and PFK expression in cytosols of L929 cells after TNF-α treatment. Results are expressed as means $\pm$ S.D. from three independent experiments. $^*P < 0.001$ between control and treated cells.

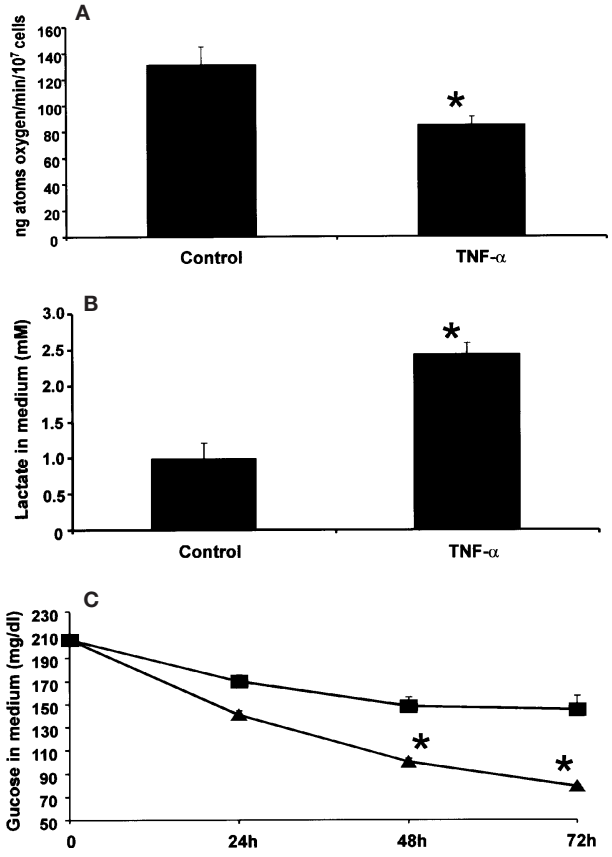

Figure 8 Effects of TNF-α on mitochondrial respiratory chain and glycolysis rate

(**A**) Effect of TNF-α on cytochrome *c* oxidase activity. L929 cells were treated for 72 h with TNF-α (25 ng/ml). Cells were then placed in an oxygen electrode cuvette. Oxygen consumption was measured using ascorbate/TMPD as the electron donor. (**B**) Effect of TNF-α on lactate production. L929 cells were treated for 72 h with TNF-α (25 ng/ml) and lactate concentration was determined in the medium samples as described in the Experimental section. (**C**) Effect of TNF-α on glucose consumption. L929 cells were treated for 72 h with TNF-α (25 ng/ml) and glucose concentration, at the indicated times, was determined in the medium from control (■) and TNF-α-treated (▲) cells as described in the Experimental section. Values are given as means $\pm$ S.D. from three independent experiments. $^*P < 0.001$ between control and experimental cells.

changes in mitochondrial transcripts, indicating that mitochondrial gene expression is regulated by TNF-α at the level of transcription and/or RNA stabilization and not by gene dosage.

Effects of TNF-α on protein levels

Having shown that TNF-α decreased mitochondrial mRNA levels and increased the mRNA levels of two key enzymes in the glycolytic pathway, we next determined whether these alterations were also reflected at the protein level. Thus we examined the protein levels of several mitochondrial proteins encoded by either the mitochondrial or the nuclear DNA, and the cytosolic GAPDH and PFK, encoded by the nuclear DNA.

Western blot analysis of the mitochondrial fraction from control and TNF-α-treated L929 cells revealed that TNF-α induced a significant decrease in the protein levels of ATPase subunit *a* and COX II, both of which are encoded by the mtDNA (Figure 6). In contrast, mitochondrial proteins encoded by the nucleus, such as cytochrome *c* oxidase, subunit IV, ubiquinol-cytochrome *c* oxidoreductase subunit core 2, ATPase subunit α and cytochrome *c*, were unaltered. These results suggest that TNF-α treatment affects mitochondria by down-regulating the expression levels of proteins encoded by the mtDNA. To verify the functional significance of the increased mRNA steady-state levels of key glycolytic enzymes at the protein level, we also performed Western blot analysis of cytosolic fractions from control and TNF-α-treated L929 cells (Figure 7). TNF-α induced a significant increase in the protein levels of PFK, whereas the levels of GAPDH were unaltered. These results were confirmed by measuring the enzymic activity for both proteins in whole-cell lysates (results not shown). Furthermore, the protein levels of MnSOD, a mitochondrial protein involved in antioxidant defence and encoded by the nucleus, were increased after TNF-α treat-

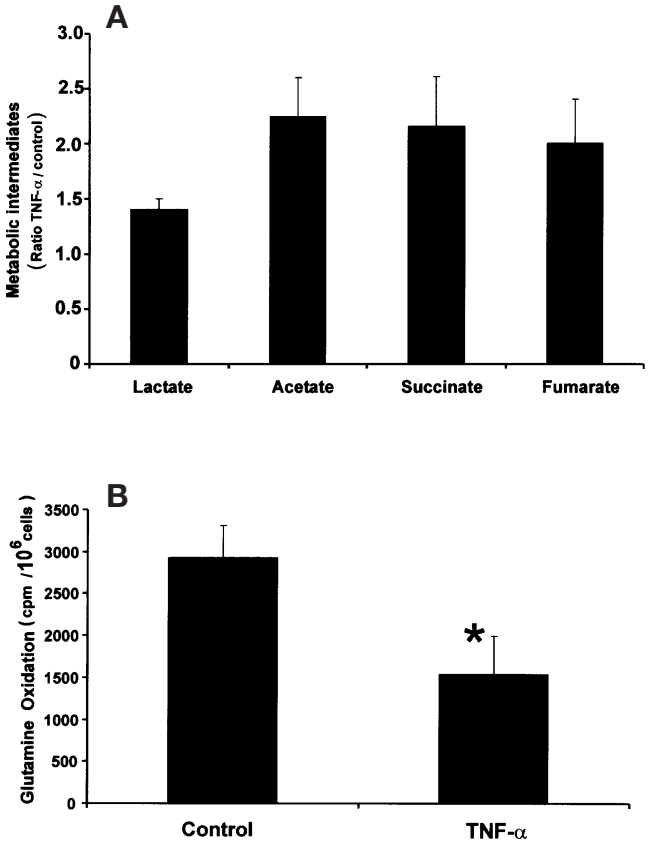

Figure 9 Effects of TNF-α on the catabolic function of the TCA cycle

(**A**) Effect of TNF-α intracellular metabolic intermediates. Cellular extract from L929 cells treated with TNF-α (25 ng/ml) for 72 h were subjected to ^{1}H-NMR analysis as is described in the Experimental section. Results are expressed as the means ± S.D. of the ratio TNF-α/control values of three independent experiments. (**B**) Effect of TNF-α on glutamine oxidation. L929 cells were treated for 72 h with TNF-α (25 ng/ml). Cells were then incubated for 3 h with 0.5 μCi of L-[U-^{14}C]glutamine and the radioactive CO_2 release was trapped and measured as is described in the Experimental section. Values are given as means ± S.D. from three independent experiments. Results are expressed as c.p.m./10^6 cells. $^*P < 0.001$ between control and treated cells.

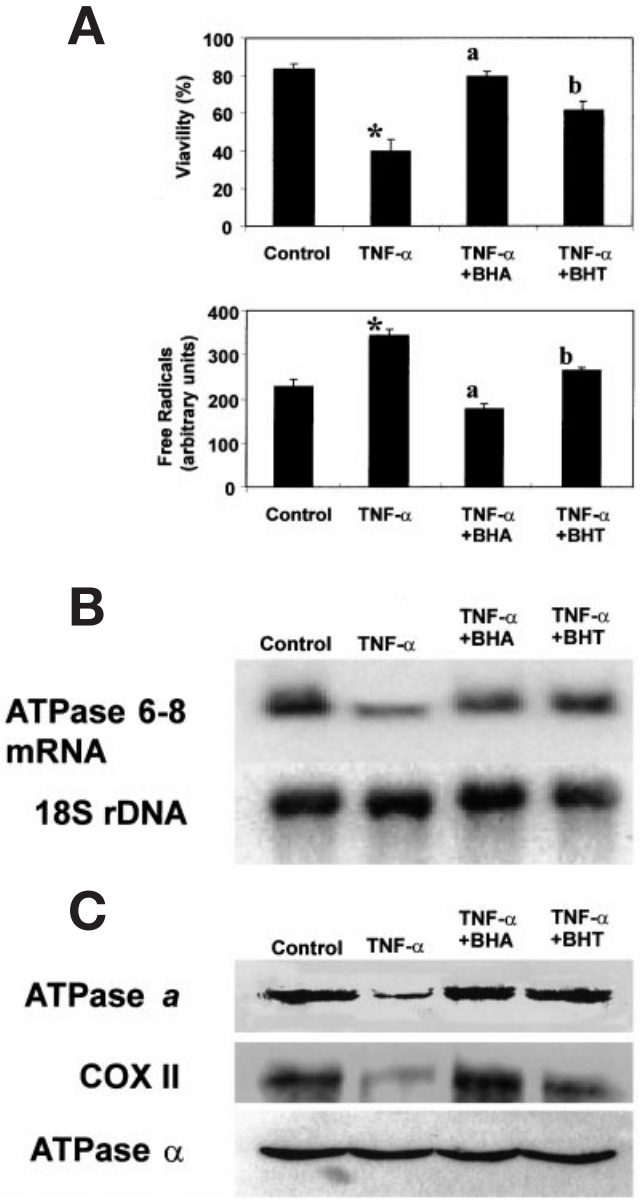

Figure 10 Effects of antioxidants on TNF-α-mediated oxidative stress

(**A**) Effect of the antioxidants BHA and BHT on TNF-α-induced cytotocicity and ROS formation. L929 cells were treated for 72 h with TNF-α (25 ng/ml). BHA (40 μM) or BHT (100 μM) was added at the same time as TNF-α. Cell viability was examined by flow cytometry and PI staining. Cellular generation of ROS was determined by flow cytometry using R123 fluorescence. $^*P < 0.001$ between control and treated cells; $^aP < 0.001$ and $^bP < 0.01$ between TNF-α and TNF-α/BHA or TNF-α/BHT respectively. (**B**) Effect of the antioxidants BHA and BHT on TNF-α-induced down-regulation of the mitochondrial transcript ATPase 6-8. Total RNA (10 μg/lane) isolated from control and TNF-α-treated (25 ng/ml) L929 cells for 72 h in the absence or presence of BHA (40 μM) or BHT (100 μM), was analysed by Northern hybridization using a radiolabelled ATPase 6-8 probe. RNA loading and integrity was assessed by probing with 18 S rDNA. (**C**) Effect of the antioxidants BHA and BHT on TNF-α-induced down-regulation of mitochondrial protein levels. Proteins from mitochondrial extracts of L929 cells exposed to TNF-α (25 ng/ml) in the presence or absence of BHA or BHT were separated by SDS/PAGE (10% gel) and immunostained with antibodies against ATPase subunits *a* and α, and COX II.

ment, indicating that TNF-α also triggers the induction of protective mechanisms against ROS.

Mitochondrial dysfunction and shift from oxidative phosphorylation to glycolysis

To determine mitochondrial dysfunction and the compensatory glycolytic pathway shift under TNF-α treatment, we measured cytochrome *c* oxidase activity, lactate production and glucose consumption in control and TNF-α-treated cells for 72 h. TNF-α induced a significant decrease in cytochrome *c* oxidase activity and a substantial increase in lactate production and glucose consumption (Figure 8). These results confirmed that mitochondrial dysfunction led to a compensatory increase in the glycolytic flux in L929 cells. To further analyse the metabolic alterations induced by TNF, we performed ^{1}H-NMR analysis of cellular extracts from L929 cells treated with TNF for 72 h. We observed that TNF-α induced the intracellular accumulation of lactate, acetate and several metabolic intermediates from the tricarboxylic acid (TCA) cycle such as fumarate and succinate (Figure 9A). To confirm the TCA cycle dysfunction at this time, we also measured glutamine oxidation in control and TNF-α-treated cells for 72 h. As is shown in Figure 9(B), glutamine oxidation was significantly decreased in TNF-α-treated cells, suggesting a blockade of the TCA cycle.

Although substantial changes in mitochondria function were observed after 72 h of TNF-α treatment, no significant change in ATP content was observed in TNF-α-treated cells compared with that of the control cells (8.0 ± 1.45 versus 8.40 ± 1.6 nmol/10^6 cells), suggesting that the compensatory increase in the glycolytic flux was able to maintain cellular ATP levels in the majority of living cells.

Antioxidants blocked the decrease in ATP 6-8 mRNA levels

To further examine the role of ROS generation in both the TNF-α-induced cytotoxicity, and down-regulation of mitochondrial transcripts and proteins, we treated the cells with TNF-α in the presence of two antioxidants, BHA and BHT, and examined the rate of cell death, ROS levels, steady-state levels of ATPase 6-8 mRNA and protein levels of several mitochondrial proteins. Both antioxidants attenuated cell death, blocked ROS generation, prevented the down-regulation of the mitochondrial transcript ATPase 6-8 and preserved the protein levels of both ATPase subunit *a* and COX II (Figure 10). These results suggest that TNF-α-induced ROS production in L929 cells may be involved in the down-regulation of mtDNA transcription or mitochondrial mRNA stability, the reduced expression level of mitochondrial proteins encoded by mtDNA and in cell death. To further support the role of ROS formation and ATPase 6-8 down-regulation in TNF-α-induced cytotoxicity, we followed the kinetics of both phenomena in human MRC-5 fibroblasts and rat hepatic stellate cells, two TNF-α-resistant cell lines. In these cells, neither ROS production nor ATPase 6-8 down-regulation was observed (results not shown), suggesting their connection with TNF-α cytotoxicity.

DISCUSSION

To explain the mechanism of TNF cytotoxicity, we studied the pathological changes induced by this cytokine in L929 cells and the protective mechanism activated by the cells to survive. First, we showed that TNF-α-induced necrosis in L929 cells was associated with increased ROS production and decreased glutathione levels. These results are in agreement with numerous studies that have previously reported that TNF-α induces ROS production, presumably at the mitochondrial level [7–9,41]. The observation that mitochondria are the main source of ROS in TNF-α cytotoxicity also suggests that mitochondrial components may be especially sensitive to oxidative damage. However, the real target of the ROS effect remains unclear. Several studies have shown that mitochondrial RNAs undergo specific degradation in different models of oxidative stress. Following treatment of hamster fibroblasts with H_2O_2, Crawford et al. [27] observed that the 16 S rRNA, a major component of mitochondrial ribosomes, was specifically degraded whereas cytosolic mRNA was not. This resulted in a dramatic shutdown of mitochondrial protein biosynthesis. A similar observation was reported in a human megakaryocyte cell line, where endogenous H_2O_2 leads to a decrease in mitochondrial RNA levels [42]. In addition, oxidative stress caused by H_2O_2 treatment, catalase knock-out or aging has been reported to be closely associated with reductions in mitochondrial transcripts and contributes to mitochondrial dysfunction in *Drosophila melanogaster* [43,44]. Consistent with these results, we demonstrated that TNF-α induced a down-regulation of the mitochondrial transcript ATPase 6-8 and other mitochondrial transcripts detected by the pAM I probe. This alteration at the RNA level was associated with a decrease in protein levels of the ATPase subunit *a*, which is encoded by the bicistronic mRNA ATPase 6-8. Furthermore, TNF induced a down-regulation of protein levels of other mitochondrial proteins encoded by the mtDNA, such as COX II. Together, these results suggest that TNF-α had a general effect on the steady-state levels of mitochondrial transcripts and mtDNA-encoded proteins. The F_1F_0-ATPase or F_1F_0-ATP synthase is the key enzyme for ATP production in mammals [45]. It catalyses ADP phosphorylation using an electrochemical proton gradient generated by the mitochondrial electron-transport chain [46]. It is a ubiquitous, highly conserved enzyme composed by two main sectors: F_0, which is membrane-embedded and comprises 10 different subunits, and F_1, which is an extrinsic-membrane catalytic sector containing five subunits. All components are required to obtain functional ATP synthase. A large body of evidence supports the notion that reversible ATP synthesis coupled to a proton flux across F_0 is mediated by conformational changes transmitted from the membrane sector to the catalytic sector of the F_0F_1 complex. The ATPase subunit *a* protein is a component of sector F_0. The subunits of F_0 together provide the proton-conduction pathway and mutagenesis studies have indicated that ATPase subunit *a* is important for proton transport [47]. ATPase subunit *a* down-regulation should therefore invariably slow down mitochondrial ATP synthesis and block or slow down the intermediary metabolism.

As the terminal component of the mitochondrial respiratory chain, cytochrome *c* oxidase catalyses the transfer of electrons from reduced cytochrome *c* to molecular oxygen and utilizes the free energy of this reaction to sustain a transmembrane proton gradient which is then used to drive the synthesis of ATP or ion transport [48]. Mammalian cytochrome *c* oxidase contains a total of 10 nuclear-encoded and three mitochondrially encoded polypeptide subunits. Subunits I (COX I) and II (COX II) are the catalytic core of the enzyme. Subunit III and most of the nuclear subunits are essential for the assembly of a functional catalytic enzyme [49]. Thus the reduced protein levels of COX II and ATPase subunit *a* may have important functional consequences and would explain the mitochondrial dysfunction induced by TNF-α, which has been characterized in many reports [7,9,50]. In fact, we demonstrated that TNF-α treatment induced a significant reduction in cytochrome *c* oxidase activity and glutamine oxidation, indicating that the normal electron flux in mitochondria is altered. However, despite significant changes in mitochondria function were observed in TNF-treated cells, the cellular ATP content did not change significantly, which may be explained by the adaptive changes in the energy-generation mechanism activated in these cells. When the reduced oxidative ability caused by TNF-α treatment cannot meet the cellular requirements for energy, up-regulation of glycolysis may occur, as demonstrated previously in different experimental models [51]. Indeed, we observed a shift from oxidative phosphorylation to glycolysis in TNF-α-treated cells, as demonstrated by significantly increased lactate production and glucose consumption in these cells. Supporting this hypothesis, we demonstrated that simultaneously to mitochondrial mRNA and protein down-regulation, TNF-α also induced an up-regulation of the steady-state mRNA levels for GAPDH and PFK. This increase was associated with increased protein levels of PFK, a key enzyme in glycolysis. Taken together these observations suggest that L929 cells attempt to compensate for the TNF-α-induced down-regulation of mitochondrial gene and protein expression by stimulating the expression of glycolytic enzymes, and thus, increasing the glycolytic flux.

There are three possibilities to explain the down-regulation of the mitochondrial transcripts: (i) reduced gene dosage, (ii) reduced transcription rate and (iii) increased degradation of mitochondrial transcripts. We showed that TNF-α had no effect

on mtDNA content, suggesting that reduced gene dosage is probably not the cause of mitochondrial mRNA down-regulation. Furthermore, the absence of smearing of the bands suggested that the decrease in the mitochondrial mRNA levels is probably due to a reduced transcription rate and not degradation.

Several reports have implicated ROS production in TNF-α-induced cytotoxicity on the basis of the protective effects exerted by radical scavengers [7,9]. We show here that the radical scavengers BHA and BHT blocked the production of free radicals, prevented the down-regulation of ATPase 6-8 transcripts, preserved the protein levels of ATPase subunit *a* and COX II, and attenuated the cytotoxic response to TNF-α, suggesting a direct link between these alterations.

In summary, we have shown that TNF-α-induced necrosis in L929 was associated with ROS production, down-regulation of mitochondrial transcripts and reduced protein levels of the ATPase subunit *a* and COX II, both mitochondrial proteins encoded by mtDNA. Functionally, cytochrome *c* oxidase activity and glutamine oxidation was decreased. Simultaneously, the cells promoted compensatory and protective mechanisms, such as induction of MnSOD and up-regulation of glycolytic enzymes at both the RNA and protein levels, accompanied by an increased glycolytic flux. The antioxidants BHA and BHT blocked the production of free radicals, prevented the down-regulation of ATPase 6-8 transcripts and ATPase subunit *a* expression levels, and attenuated the cytotoxic response to TNF-α, suggesting a direct relationship between these phenomena. According to this scheme, TNF-α-induced ROS production could be sufficient to override cell antioxidant defences and lead to cell death by down-regulating key components of the mitochondrial oxidative phosphorylation, consequently provoking a bioenergetic collapse if a sufficient glycolytic compensatory increase is not activated. Alternatively, the intracellular accumulation of lactate and other TCA cycle intermediates due to efficient compensatory glycolysis could alter cellular osmotic and pH homoeostasis and induce, eventually, plasma membrane permeabilization. In both hypotheses, the balance between pathological changes and protective mechanisms seems to be essential to decide the fate of cells.

This work has been partially supported by the Spanish Direccion General de Enseñanza Superior grant no. PB98-0329-C02-01 and Fondo de Investigación Sanitaria (FIS 00/373). We thank Dr Rosa Luna and Dr Andrés Aguilera (Departamento de Genética, Facultad de Biología, Universidad de Sevilla, Seville, Spain) for their help with the Northern blot analysis.

REFERENCES

1 Beutler, B. and Cerami, A. (1987) Cachectin: more than a tumor necrosis factor. N. Engl. J. Med. **316**, 379–385
2 Carswell, E. A., Old, L. J., Kassel, R. L., Green, S., Fiore, N. and Williamson, B. (1975) An endotoxin-induced serum factor that causes necrosis of tumors. Proc. Natl. Acad. Sci. U.S.A. **72**, 3666–3670
3 Fiers, W., Beyaert, R., Declercq, W. and Vandenabeele, P. (1999) More than one way to die: apoptosis, necrosis and reactive oxygen damage. Oncogene **18**, 7719–7730
4 Wallach, D., Boldin, M., Varfolomeev, E., Beyaert, R., Vandenabeele, P. and Fiers, W. (1997) Cell death induction by receptors of the TNF family: towards a molecular understanding. FEBS Lett. **410**, 96–106
5 Liu, Y., Tergaonkar, V., Krishna, S. and Androphy, E. J. (1999) Human papillomavirus type 16 E6-enhanced susceptibility of L929 cells to tumor necrosis factor α correlates with increased accumulation of reactive oxygen species. J. Biol. Chem. **274**, 24819–24827
6 Vercammen, D., Vandenabeele, P., Beyaert, R., Declercq, W. and Fiers, W. (1997) Tumour necrosis factor-induced necrosis versus anti-Fas-induced apoptosis in L929 cells. Cytokine **9**, 801–808
7 Goossens, V., Grooten, J., De Vos, K. and Fiers, W (1995) Direct evidence for tumor necrosis factor-induced mitochondrial reactive oxygen intermediates and their involvement in cytotoxicity. Proc. Natl. Acad. Sci. U.S.A. **92**, 8115–8119
8 Shoji, Y., Uedono, Y., Ishikura, H., Takeyama, N. and Tanaka, T. (1995) DNA damage induced by tumour necrosis factor-α in L929 cells is mediated by mitochondrial oxygen radical formation. Immunology **84**, 543–548
9 Schulze-Osthoff, K., Bakker, A. C., Vanhaesebroeck, B., Beyaert, R., Jacob, W. A. and Fiers, W. (1992) Cytotoxic activity of tumor necrosis factor is mediated by early damage of mitochondrial functions. Evidence for the involvement of mitochondrial radical generation. J. Biol. Chem. **267**, 5317–5323
10 Wong, G. H., Elwell, J. H., Oberley, L. W. and Goeddel, D. V. (1989) Manganous superoxide dismutase is essential for cellular resistance to cytotoxicity of tumor necrosis factor. Cell **58**, 923–931
11 Carini, R., Parola, M., Dianzani, M. U. and Albano, E. (1992) Mitochondrial damage and its role in causing hepatocyte injury during stimulation of lipid peroxidation by iron nitriloacetate. Arch. Biochem. Biophys. **297**, 110–118
12 Masumoto, N., Tasaka, K., Miyake, A. and Tanizawa, O. (1990) Superoxide anion increases intracellular free calcium in human myometrial cells. J. Biol. Chem. **265**, 22533–22536
13 Kowaltowski, A. J., Castilho, R. F. and Vercesi, A. E. (2001) Mitochondrial permeability transition and oxidative stress. FEBS Lett. **495**, 12–15
14 Cadet, J., Delatour, T., Douki, T., Gasparutto, D., Pouget, J. P., Ravanat, J. L. and Sauvaigo, S. (1999) Hydroxyl radicals and DNA base damage. Mutat. Res. **424**, 9–21
15 Collins, A. R. (1999) Oxidative DNA damage, antioxidants, and cancer. Bioessays **21**, 238–246
16 Grune, T., Reinheckel, T., Joshi, M. and Davies, K. J. (1995) Proteolysis in cultured liver epithelial cells during oxidative stress. Role of the multicatalytic proteinase complex, proteasome. J. Biol. Chem. **270**, 2344–2351
17 Wiese, A. G., Pacifici, R. E. and Davies, K. J. (1995) Transient adaptation of oxidative stress in mammalian cells. Arch. Biochem. Biophys. **318**, 231–240
18 Crawford, D. R. and Davies, K. J. (1994) Adaptive response and oxidative stress. Environ. Health Perspect. **102** (Suppl. 10), 25–28
19 Sastre, J., Pallardo, F. V., Garcia de la Asunción, J. and Vina, J. (2000) Mitochondria, oxidative stress and aging. Free Radical Res. **32**, 189–198
20 Zhang, Y., Marcillat, O., Giulivi, C., Ernster, L. and Davies, K. J. (1990) The oxidative inactivation of mitochondrial electron transport chain components and ATPase. J. Biol. Chem. **265**, 16330–16336
21 Bindoli, A. (1988) Lipid peroxidation in mitochondria. Free Radicals Biol. Med. **5**, 247–261
22 Cadenas, E. and Davies, K. J. (2000) Mitochondrial free radical generation, oxidative stress, and aging. Free Radicals Biol. Med. **29**, 222–230
23 Farber, J. L., Kyle, M. E. and Coleman, J. B. (1990) Mechanisms of cell injury by activated oxygen species. Lab. Invest. **62**, 670–679
24 Kowaltowski, A. J. and Vercesi, A. E. (1999) Mitochondrial damage induced by conditions of oxidative stress. Free Radicals Biol. Med. **26**, 463–471
25 Crawford, D. R., Abramova, N. E. and Davies, K. J. (1998) Oxidative stress causes a general, calcium-dependent degradation of mitochondrial polynucleotides. Free Radicals Biol. Med. **25**, 1106–1111
26 Elliott, R. M., Southon, S. and Archer, D. B. (1999) Oxidative insult specifically decreases levels of a mitochondrial transcript. Free Radicals Biol. Med. **26**, 646–655
27 Crawford, D. R., Lauzon, R. J., Wang, Y., Mazurkiewicz, J. E., Schools, G. P. and Davies, K. J. (1997) 16S mitochondrial ribosomal RNA degradation is associated with apoptosis. Free Radicals Biol. Med. **22**, 1295–1300
28 Crawford, D. R., Wang, Y., Schools, G. P., Kochheiser, J. and Davies, K. J. (1997) Down-regulation of mammalian mitochondrial RNAs during oxidative stress. Free Radicals Biol. Med. **2**, 551–559
29 Decker, T. and Lohmann-Matthes, M. L. (1988) A quick and simple method for the quantitation of lactate dehydrogenase release in measurements of cellular cytotoxicity and tumor necrosis factor (TNF) activity. J. Immunol. Methods **115**, 61–69
30 White, B. A. and Bancroft, F. C. (1982) Cytoplasmic dot hybridization. Simple analysis of relative mRNA levels in multiple small cell or tissue samples. J. Biol. Chem. **257**, 8569–8572
31 Eady, J. J., Orta, T., Dennis, M. F., Stratford, M. R. and Peacock, J. H. (1995) Glutathione determination by the Tietze enzymatic recycling assay and its relationship to cellular radiation response. Br. J. Cancer **72**, 1089–1095
32 Tietze, F. (1969) Enzymatic method for quantitative determination of nanogram amounts of total and oxidized glutathione: applications to mammalian blood and other tissues. Anal. Biochem. **27**, 502–522
33 Bossy-Wetzel, E., Newmeyer, D. D. and Green, D. R. (1998) Mitochondrial cytochrome c release in apoptosis occurs upstream of DEVD-specific caspase activation and independently of mitochondrial transmembrane depolarization. EMBO J. **17**, 37–49
34 Flick, D. A. and Gifford, G. E. (1984) Comparison of in vitro cell cytotoxic assays for tumor necrosis factor. J. Immunol. Methods **68**, 167–175
35 Levesque, A., Paquet, A. and Page, M. (1995) Measurement of tumor necrosis factor activity by flow cytometry. Cytometry **20**, 181–184
36 Mishra, S. (1995) A spin decay assay for tumor necrosis factor cytotoxicity. Indian J. Biochem. Biophys. **32**, 254–260

37 Trost, L. C. and Lemasters, J. J. (1994) A cytotoxicity assay for tumor necrosis factor employing a multiwell fluorescence scanner. Anal. Biochem. **220**, 149–153
38 Sanchez-Alcazar, J. A., Schneider, E., Martinez, M. A., Carmona, P., Hernandez-Munoz, I., Siles, E., De La Torre, P., Ruiz-Cabello, J., Garcia, I. and Solis-Herruzo, J. A. (2000) Tumor necrosis factor-α increases the steady-state reduction of cytochrome b of the mitochondrial respiratory chain in metabolically inhibited L929 cells. J. Biol. Chem. **275**, 13353–13361
39 Sanchez-Alcazar, J. A., Khodjakov, A. and Schneider, E. (2001) Anticancer drugs induce increased mitochondrial cytochrome c expression that precedes cell death. Cancer Res. **61**, 1038–1044
40 Allen, R. G. and Tresini, M. (2000) Oxidative stress and gene regulation. Free Radicals Biol. Med. **28**, 463–499
41 Hennet, T., Richter, C. and Peterhans, E. (1993) Tumour necrosis factor-α induces superoxide anion generation in mitochondria of L929 cells. Biochem. J. **289**, 587–592
42 Austin, R. C., Sood, S. K., Dorward, A. M., Singh, G., Shaughnessy, S. G., Pamidi, S., Outinen, P. A. and Weitz, J. I. (1998) Homocysteine-dependent alterations in mitochondrial gene expression, function and structure. Homocysteine and H2O2 act synergistically to enhance mitochondrial damage. J. Biol. Chem. **273**, 30808–30817
43 Schwarze, S. R., Weindruch, R. and Aiken, J. M. (1998) Oxidative stress and aging reduce COX I RNA and cytochrome oxidase activity in *Drosophila*. Free Radicals Biol. Med. **25**, 740–747

Received 18 October 2002; accepted 6 December 2002
Published as BJ Immediate Publication 6 December 2002, DOI 10.1042/BJ20021623

44 Calleja, M., Pena, P., Ugalde, C., Ferreiro, C., Marco, R. and Garesse, R. (1993) Mitochondrial DNA remains intact during Drosophila aging, but the levels of mitochondrial transcripts are significantly reduced. J. Biol. Chem. **268**, 18891–18897
45 Weber, J. and Senior, A. E. (2000) ATP synthase: what we know about ATP hydrolysis and what we do not know about ATP synthesis. Biochim. Biophys. Acta **1458**, 300–309
46 Boyer, P. D. (1997) The ATP synthase–a splendid molecular machine. Annu. Rev. Biochem. **66**, 717–749
47 Vik, S. B. and Antonio, B. J. (1994) A mechanism of proton translocation by F1F0 ATP synthases suggested by double mutants of the a subunit. J. Biol. Chem. **269**, 30364–30369
48 Hatefi, Y. (1985) The mitochondrial electron transport and oxidative phosphorylation system. Annu. Rev. Biochem. **54**, 1015–1069
49 Wikstrom, M. (1998) Cytochrome oxidase: structure and mechanism. Foreword. J. Bioenerg. Biomembr. **30**, 3–5
50 Schulze-Osthoff, K., Beyaert, R., Vandevoorde, V., Haegeman, G. and Fiers, W. (1993) Depletion of the mitochondrial electron transport abrogates the cytotoxic and gene-inductive effects of TNF. EMBO J. **12**, 3095–3104
51 Li, Y. Y., Chen, D., Watkins, S. C. and Feldman, A. M. (2001) Mitochondrial abnormalities in tumor necrosis factor-α-induced heart failure are associated with impaired DNA repair activity. Circulation **104**, 2492–2497